J Nanopart Res (2011) 13:4253Ð4266
DOI 10.1007/s11051-011-0369-0

RESEARCH PAPER

Nanoparticle mixing through rapid expansion of high pressure and supercritical suspensions

Daniel To € Sankaran Sundaresan€ Rajesh Dave

Received: 30 August 2010 / Accepted: 29 March 2011 / Published online: 12 April 2011
Springer Science+Business Media B.V. 2011

Abstract Mixing of binary mixtures of nanopowders afforded by rapid expansion of high pressure and supercritical suspensions (REHPS) is investigated to examine the roles of two previously reported deagglomeration mechanisms. The quality of mixing was characterized through intensity and scale of segregation using concentration data obtained through energy dispersive X-ray spectroscopy; the corresponding deagglomeration was quantiÞed using differential mobility and image analyses in conjunction with electron microscopy. Increasing the pressure from which expansion was carried out, and decreasing the nozzle diameter led to improved deagglomeration. However, increased pressure alone did not inßuence the mixture quality, which was found to also depend on the scale of mixedness of the constituents before transport through the nozzle, establishing that the REHPS mixing is signiÞcantly improved by improving the quality of the premix. The scale of segregation correlated with the size of the most energetic eddies present during ßow through the nozzle, both of which increased with nozzle diameter, corroborating the importance of previously reported shear-induced deagglomeration mechanism. Finally, REHPS was also shown to be capable of deagglomerating carbon nanotube bundles and mix them well with alumina, silica, and titania at submicron scale.

Keywords Nanomixing · Nanoparticles · Supercritical ßuids · Rapid expansion · Intensity of segregation · Carbon dioxide · Carbon nanotubes

Introduction

Nano-composite materials, where two or more constituents are mixed together at the nanoscale, often manifest superior properties over systems where they are mixed on the macroscale (Sun et al. 2005; Kumari et al. 2008; Sperling and Parak 2010; Duncan and Rouvray 1989; Rawle 2007; Shinohara et al. 1986; VolÕkhin et al. 2000; Sanganwar and Gupta 2008; Shieh et al. 2005). Although nano-composites may be directly produced in some applications, in many instances such composites are fabricated by mixing the individual constituents, followed by pressing and sintering. As dry nanoparticles readily form large loose (often fractal) agglomerates (Nakamura and Watano 2008; Nam et al. 2004; Valverde et al. 2008; Wei et al. 2002), mixing the individual constituents at the nanoscale (or even a submicron scale) in a dry

D. To · R. Dave (✉)
Otto York Department of Chemical, Pharmaceutical and Biological Engineering, New Jersey Institute of Technology, University Heights, Newark, NJ 07102-1982, USA
e-mail: dave@adm.njit.edu

S. Sundaresan
Department of Chemical and Biological Engineering, Princeton University, Princeton, NJ 08544, USA

state is difficult; mixing only at a coarser (i.e., agglomerate) scale results in low-quality composites (Shinohara et al. 1986; Volokhin et al. 2000; Sanganwar and Gupta 2008; Shieh et al. 2005). Conventionally, the mixing of nanomaterials is performed in liquid solvents with other additives (salts and surfactants); however, considerable effort is in progress to achieve improved mixing of multicomponent nanopowders in a dry state. Some of these methods include magnetically assisted impact mixing (Wei et al. 2002; Yang et al. 2003), microjet-assisted fluidization (Quevedo et al. 2009) and other enhanced fluidization techniques (Huang et al. 2008; Nakamura and Watano 2008), ultrasonication in supercritical fluids (Sanganwar et al. 2008), and rapid expansion of high pressure and supercritical suspensions (REHPS) (To et al. 2009; Wei et al. 2002; Yang et al. 2003). This study is concerned with REHPS, where CO_2 is used as an environmentally benign solvent.

Coarse-scale mixing of the nanopowders can be achieved through mild handling, such as fluidization, capable of deagglomeration on the scale of 20–30 μm and therefore mixing on a comparable scale (Nakamura and Watano 2008; Ammednola and Chiron 2010). It is readily apparent that the first step in achieving mixing at a finer scale is deagglomeration. The effectiveness of REHPS in deagglomerating nanoparticle agglomerates (henceforth simply referred to as nanopowders) has already been demonstrated by To et al. who expanded suspensions of nanopowders in high pressure and supercritical carbon dioxide through capillary nozzles (To et al. 2009). This process is similar in principle to the liquid-phase dispersion process commonly referred to as high-pressure homogenization with the exception being that a compressible gaseous or supercritical medium is used, and therefore requires very different experimental practices. In both methods, a suspending fluid carrying nanopowders is throttled through a fine-capillary nozzle; high-shear/energy dissipation rates inside and at the entrance to the nozzle are expected to cause agglomerate breakage (To et al. 2009; Endo et al. 1997; Galinat et al. 2005; Perry and Green 2009; Pope 2000; Seekkuarachchi and Kumazawa 2008; Strecker and Roth 1994; Vankova et al. 2007; Voss and Finlay 2002; Zumaeta et al. 2005, 2007). The use of gaseous and supercritical CO_2 in REHPS takes advantage of its liquid-like density, gas-like viscosity, and compressibility in the homogenization process and results in three major beneficial differences:

(1) Pressures lower than 20 MPa are commonly used in the REHPS process (To et al. 2009; Wei et al. 2002; Yang et al. 2003), whereas pressures in excess of 50–500 MPa are commonly used in liquid-phase high pressure homogenization (Baldyga et al. 2007; Hu et al. 2004; Xie et al. 2008).

(2) At the exit of the nozzle, a Mach disc or shockwave forms, which has been shown to be effective in agglomerate breakup (Brandt et al. 1987; Strecker and Roth 1994). The Mach disc represents a discontinuous change in the fluid pressure, density, and velocity. It has been shown that the Mach disc can form when the ratio between the upstream and downstream pressures is as low as four. At lower-pressures ratios, weaker compression waves form (Adamson and Nicholls 1958).

(3) A high-quality dry powder mixture can be collected directly after REHPS without drying steps that lead to caking or segregation. A similar benefit can be observed for liquid carbon dioxide as well, as it readily evaporates at atmospheric conditions.

The feasibility of the REHPS process for deagglomeration and mixing of nanopowders has been reported in the literature (Wei et al. 2002; Yang et al. 2003; To et al. 2009). Wei et al. (2002) presented the results of a single experiment on REHPS mixing and thus established the proof-of-concept. Yang et al. (2003) showed that the REHPS process was capable of mixing nanopowders on the submicron scale; however, only limited experimental conditions were investigated. To et al. (2009) recently performed detailed studies on deagglomeration of alumina and titania nanopowders and reported a systematic effect of pressure on deagglomeration efficiency: But they only reported a single REHPS mixing experiment. These authors examined two deagglomeration mechanisms; shearing in the nozzle and passing through the Mach disc at the exit of the nozzle. It was suggested that when deagglomeration occurred predominantly through shear inside the nozzle, the resulting agglomerate sizes should follow a square root dependence on the nozzle diameter; on the other hand, if deagglomeration occurred principally at the

Mach disc, the average size of the deagglomerated fragments would decrease with increasing upstream pressure, but be unaffected by nozzle diameter. However, these models have not yet been compared with experimental data. *The first objective* of this study is to test the relative importance of these two mechanisms experimentally. It should be noted that Yang et al. (2003) undertook a limited study of nanopowder mixing using the REHPS process and did not find a significant influence of the nozzle diameter. However, in these studies (Wei et al. 2002; Yang et al. 2003), constant upstream pressure was not maintained during expansion, and the upstream pressure decreased by nearly 30% during the experiment; this complicates testing of the deagglomeration mechanism. Indeed, we demonstrate in this study that a systematic effect of the nozzle diameter is observed when the upstream pressure is maintained constant during the course of an experiment.

The second objective is to undertake a systematic study of the influence of processing conditions on the quality of mixing achieved in REHPS. Previous studies carried out limited explorations of the mixing quality. Yang et al. (2003) characterized the mixing quality by comparing elemental ratios at 20 random points from a single loose powder sample through energy dispersive X-ray spectroscopy (EDS), which is limited in scope. In contrast, this study employs a more rigorous characterization of the mixing quality through analysis of the *intensity and scale of segregation* (Danckwerts 1952). Both of these analyses measures strongly depend on the length scale of scrutiny. If a mixture is investigated at too fine a length scale, it appears completely segregated; on the other hand, when a very coarse scale of scrutiny is used, it appears completely homogeneous (Van der Wel 1999; Venables and Wells 2001; Danckwerts 1952). As a result, the scale of segregation can be used to characterize coarse-scale mixtures, but offers limited value for high-quality mixtures. Oppositely, the intensity of segregation can differentiate between high-quality mixtures, but offers limited value for low-quality mixtures. In this study, we differentiate between multiple high-quality mixtures through the intensity of segregation (Sanganwar et al. 2008; To et al. 2009; Scicolone et al. 2008) determined using EDS results at 400 random points on the smooth surface of a tableted powder sample. Coarse-scale mixtures are characterized by the scale of segregation of EDS-based maps on elemental concentration with respect to spatial locations, which is a novel addition to the analysis of nanopowders mixtures. This study also follows a more rigorous mixing experimental protocol than the previous studies (Wei et al. 2002; Yang et al. 2003). First, the preexpansion pressure is held constant during the experiments. Next, we systematically vary the nozzle diameter, the conditions from which the expansion is carried out, and the method of premixing the agglomerates of the individual constituents. Through such studies, the influence of several important variables on nanomixing is examined, namely, the state of premixing of the agglomerates of the individual constituents, the nozzle size, and the upstream pressure. It has been demonstrated in this study that the more tightly controlled mixing experiment protocols and rigorous characterization methods have permitted a better understanding of the deagglomeration mechanisms and the nanomixing through the REHPS process.

The third objective is to explore potential applications of REHPS in creating nano-composites, which have not been reported in previous studies. The first application is on formation of mullite, an aluminosilicate valued for its refractory properties, where we analyze the influence of the quality of mixing of a binary mixture of alumina and silica on the degree of subsequent reactive formation of mullite in a high-temperature environment. The second application examines preparation of composites containing carbon nanotubes (CNT) mixed at the submicron scale with nanopowders of alumina, silica, and titania, where the REHPS process is used for the first time to deagglomerate the carbon nanotube bundles and achieve the desired mixing.

Experimental

Alumina Aeroxide Alu C ($d_p = 13$ nm), titania P25 ($d_p = 21$ nm), silane-coated silica Aerosil R972 (i.e., hydrophobically coated, $d_p = 16$ nm; supplied by Evonik Degussa GmbH, Parsippany, NJ, USA), and multiwalled carbon nanotubes (supplied by Cheap Tubes, Inc., Brattleboro, VT, USA) were used in this study.

The experimental apparatus used in deagglomeration studies is shown in Fig. 1 (*parts I and II*). Typically, 0.1 g of nanopowder (i.e., agglomerates of nanoparticles) was charged into a 24-mL chamber

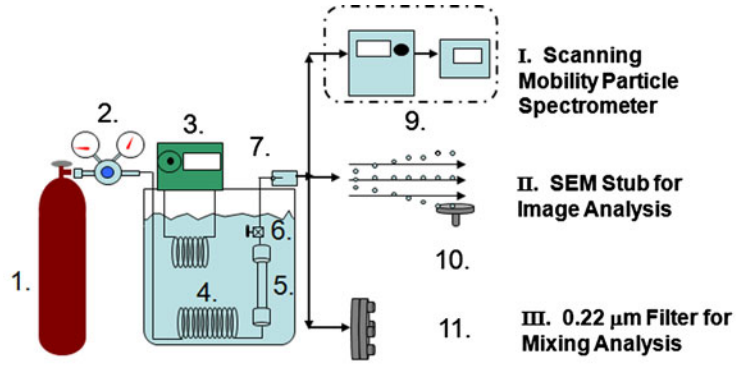

1. CO2 supply, 2. One-Stage Reducing Regulator, 3. Immersion heater and water bath, 4. heat exchange coil, 5. High pressure mixing vessel, 6. On/Off valve, 7. Capillary nozzle, 8. Expansion tube, 9. SMPS, 10. SEM stub for image analysis, 11. 0.22 μm filter.

Fig. 1 Schematic of REHPS process. Individual nanopowders expanded through the REHPS process were sized using a scanning mobility particle spectrometer and collected by diffusion and image analysis of electron micrographs. Mixed nanopowders expanded through the REHPS process were collected on a 0.2-μm filter for mixing quality analysis using energy dispersive X-ray spectroscopy

(Fig. 1, unit 5) and pressurized with CO_2 (99.9% pure, Welco Gas) to the desired operating pressure using a single-stage reducing regulator (unit 2, range 1.72–7.93 MPa). Before entering the chamber, the CO_2 was passed through a 2-m × 1.5-mm ID stainless steel heat exchange coil (unit 4) submerged in a warm water bath and immersion heater (unit 3) to transition the CO_2 into the gaseous or supercritical region and also regulate the operating temperature. More extreme conditions (i.e., pressures more than 7.93 MPa and temperatures less than the supercritical point) were not investigated as CO_2 condensation occurs on gas expansion, which was observed to lead to unrepresentative size distributions (To et al. 2009). The powders were expanded to the atmospheric pressure through a capillary nozzle (unit 7). The aerosol downstream of the nozzle was characterized online by the scanning mobility particle spectrometer (SMPS) (unit 9) (TSI, Inc., St. Paul, MN, USA), which uses differential mobility analysis to determine the size of agglomerates in the size range of 19.5–572.5 nm. The size range measured by the SMPS was 19.5–572.5 nm; the data reported in the following represent the average of nine scans for each sample. Aerosol samples were also collected by diffusion on a silicon substrate (unit 10) and were characterized offline by image analysis of electron micrographs at a magnification of 33,000. The images were processed with ImageJ, an open-source image-processing program developed by Wayne Rasband and the NIH, to determine the projected area diameter of the agglomerates (size range: 40–3,000 nm). In the case of CNTs (with high-aspect ratios), the largest end-to-end lengths of the agglomerates (Feret diameter) were determined from the electron micrographs. Typically, 1,000–2,000 agglomerates were sized through image analysis for each experiment. For a detailed description of the operating procedures of deagglomeration and characterization, refer to To et al. (2009).

The REHPS mixing apparatus is similar to the REHPS deagglomeration apparatus and is shown in Fig. 1 (*part III*). Typically, 0.75-g batch of premixed alumina and silica nanopowders was charged into the 24-mL tubular mixing chamber (unit 5). Two powder premixing methods were employed: (1) hand mixing/shaking in a 65-mL glass jar and (2) stirring a 7.0-g batch of powder at 2,000 RPM with a four-blade rotor with 1-cm blades, in supercritical CO_2 at 14.8 MPa and 35°C in a 300-L stainless steel vessel. Rapid expansion through the nozzle (254-μm ID and 10-cm long, unit 7) was conducted from different conditions upstream of the nozzle: (i) 1.72–5.51 MPa and 45 °C (where CO_2 is a high-pressure gas), (ii) 7.93–13.79 MPa and 45°C (supercritical CO_2), and (iii) 8.27 MPa and 28 °C (liquid CO_2). Pressures greater than 7.93 MPa were achieved using a liquid CO_2 pump (P-350, Thar Technologies, Pittsburgh,

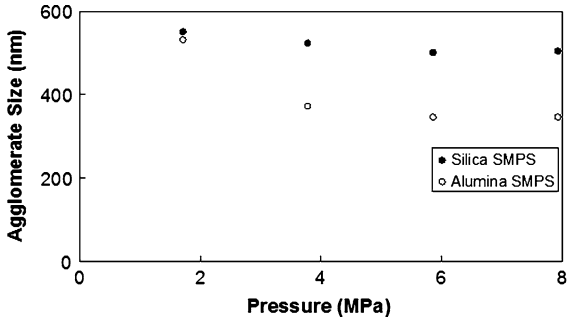

Fig. 2 Volume-weighted diameters of silica and alumina nanopowders deagglomerated (separately) through the REHPS process from various pressures. Sizes were measured with the scanning mobility particle spectrometer (range of 25Ð572 nm) (To et al. 2009)

PA, USA). The expanded mixture was collected on a 0.22-μm Þlter (Fig. 2, unit 11). Some experiments were also repeated using 508- and 1,524-μm nozzles.

The effect of multiple processing cycles on the mixture quality was also examined. Samples collected after a 1-pass REHPS were processed through REHPS (using the same procedure as earlier) for a second time at the same upstream pressures and temperatures and analyzed.

Alumina and silica with two different weight ratios, 50:50 and 71.8:28.2 (mullite stoichiometry), were subjected to REHPS mixing. The product mixtures were pressed at 600 MPa into a 13-mm tablet (0.2 g of powder was pressed) and characterized using a Þeld emission scanning electron microscope (FESEM) in conjunction with energy dispersive X-ray spectroscopy (SEMÐEDS, LEO 1530vp Gemini), which can determine the elemental composition at various spatial locations (with resolution of approximately 2 μm) (Sanganwar et al. 2008). Three replicates were prepared for each experiment and mixture qualities in the form of intensities of segregations (IOS, deÞned in the following) were averaged. Mullite stoichiometry specimens were pressed into a pellet at 600 MPa and Þred at 1,400°C for 1 h at a heating rate of 20°C/min for the purpose of producing mullite. The sintered pellets were ground with a mortar and pestle and mixed with 40 mg of CaF_2, an internal standard for X-ray powder diffraction (XRD, PW3040, Philips). The degree of mullitization was determined through quantitative XRD (by comparing the ratio of the area for the mullite peak at 25.92θ to that of the CaF_2 peak at 47.02θ to a previously prepared calibration curve). The calibration curve was prepared by comparing the peak area ratio to the mass ratio of the mullite to CaF_2.

Poor mixtures were described by the scale of segregation with a scale of scrutiny of the EDS mapping (75 × 50 μm^2). We were able to ascertain that REHPS decreased the scale of inhomogeneity substantially, as illustrated later in this manuscript; therefore, high-quality REHPS mixtures were described by the intensity of segregation with a scale of scrutiny equal to the resolution limit (1 spot, ~2 μm). It immediately follows that this approach cannot be used to distinguish between good mixtures less than the scale of scrutiny.

The EDS analysis was performed using two methodologies: (1) A scanning mode was used to produce 75 × 50 μm^2 (512 × 386 $pixel^2$) elemental mappings of the mixtures, which was used to determine the scale of segregation (SOS), with a scale of scrutiny equivalent to the dimension of the scan; (2) the elemental compositions at 400 spots (~2 μ, the scale of scrutiny), which were used to determine the intensity of segregation (IOS). High-quality REHPS mixtures were described by the intensity of segregation, which has been employed in previous studies (To et al. 2009; Sanganwar et al. 2008; Scicolone et al. 2008), whereas poor mixtures were described by the scale of segregation.

The IOS is a measure of concentration homogeneity, represented by the ratio of the concentration variance of the mixture to that of a completely segregated mixture as shown in Eq. 1, where σ^2 is the variance of the concentration between the 400 points and μ_A and μ_S are the mean values of the concentrations of alumina and silica, respectively. The product of the mean concentrations, $\mu_A\mu_S$, represents the variance of a completely segregated mixture (Weinekotter and Gericke 2000). The intensity of segregation ranges from 0 to 1, representing the completely homogeneous state and the completely segregated state, respectively.

$$\mathrm{IOS} = \frac{\sigma^2}{\mu_A \mu_S}. \qquad (1)$$

The scale of segregation (SOS) uses the autocorrelation function to determine the rank-order characteristic size of the segregated regions and is described by Eqs. 2 and 3:

$$R(r) = \sum_{i}^{N} \frac{(a_i - \bar{a})(a_{i+r} - \bar{a})}{(a_i - \bar{a})^2} \quad (2)$$

$$\mathrm{SOS} = \int_0^1 R(r)dr - \int_0^{\varepsilon} R(r)dr. \quad (3)$$

The autocorrelation function, $R(r)$, evaluates the similarity of concentrations, a_i, between two spatial locations (i and $i + r$) separated by a known distance, r, for all N combinations of coupled locations. SOS, shown in Eq. 3, represents the length scale above which the mixture can be considered random, where ε is a length scale significantly greater than the distance where $R(r) \sim 0$ (i.e., the mixture is uncorrelated). Therefore, the scale of segregation is 0 when the mixture is a completely random mixture (essentially homogeneous), and higher values suggest poorer mixtures. Here, elemental concentration was inferred from pixel brightness obtained from the EDS elemental map and the separation distance was inferred from a pixel location, which has a linear dimension of 0.15 μm/pixel.

Individual mixtures of 50 wt% of CNT with alumina, silica, and titania were also produced by 1-pass REHPS and the mixtures were only analyzed qualitatively through SEM imaging.

Results and discussion

Deagglomeration of silica nanopowders by REHPS process

The volume-weighted mode diameters for deagglomerated silica nanopowders, evaluated through the SMPS and image analysis of electron micrographs, are shown in Figs. 2 and 3, respectively. Similar results for alumina, reported in an earlier study (To et al. 2009), are also reproduced in these figures for comparison. The upstream pressure ranged from 1.72 to 7.93 MPa. The mode sizes extracted from the SMPS show a slight decrease in agglomerate size with increasing pressure, which is consistent with previous findings for alumina. A similar trend of decreasing agglomerate sizes with increasing pressure was also seen in the image analysis results presented in Fig. 3. It was observed that the sizes of the silica agglomerates were near the upper limit of the SMPS size range (19.5–572.5 nm). As both measurements revealed a decrease in agglomerate size with increasing pressure, it is reasonable to conclude that by increasing the upstream pressure, one can increase the extent of fragmentation of the agglomerates. This coincides with previous predictions that expansion from higher pressures is expected to produce smaller agglomerate sizes, as a larger portion of the mass flow passes through a more powerful Mach disc at these higher pressures and therefore produces more fines. The SMPS size results, which were primarily used to characterize the fine fraction of the size distribution, indicated that the fines are indeed getting smaller with increasing pressure. The SEM size results showed that the coarse fraction decreased with increasing pressure.

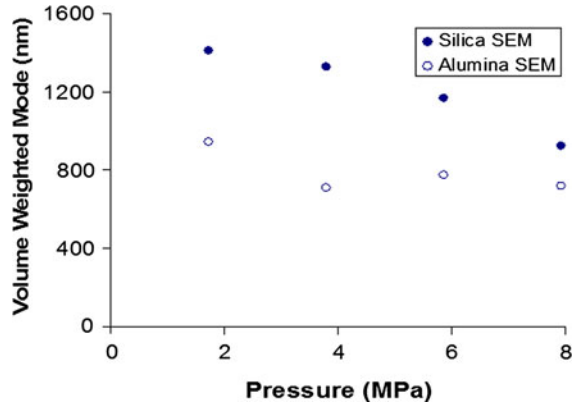

Fig. 3 Volume-weighted diameters of silica and alumina nanopowders deagglomerated (separately) through the REHPS process from various pressures. The agglomerates collected by diffusion and imaged at 33,000× with electron microscopy were analyzed to determine the sizes. Measurable sizes ranged from 40 to 3,000 nm (To et al. 2009)

As previously mentioned, expansion pressures were kept at or less than 7.93 MPa to avoid dry ice precipitation, which appears to prevent agglomerate breakup by encasing the agglomerates in a dry ice particle. Evidence of this is shown in Fig. 4, where REHPS-deagglomerated silica nanopowders expanded from 11.03 MPa and 45°C are depicted; numerous silica agglomerates were apparently trapped in a single dry ice particle, which was then deposited on the silicon wafer during expansion. As the CO_2 sublimated, the agglomerates were deposited in the configuration shown.

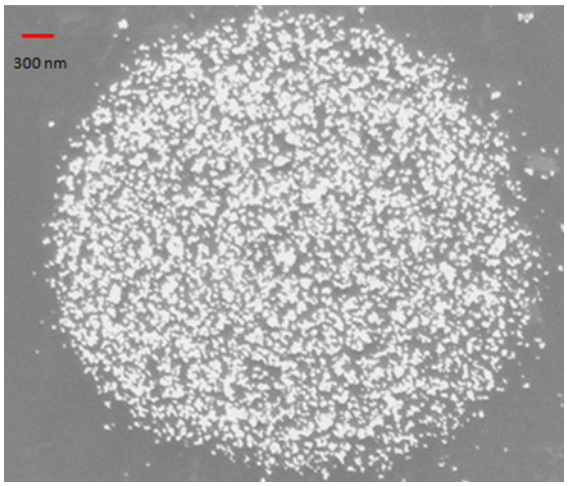

Fig. 4 SEM image of silica deagglomerated from 11.03 MPa and 45 C. It appears that dry ice precipitation during expansion from high pressures prevented effective deagglomeration

REHPS mixing of alumina–silica mixtures

The intensities of segregations obtained after various mixing protocols for alumina and silica nanopowder mixtures at weight ratios of 50:50 and 72:28 (mullite stoichiometry) are tabulated in Table 1; the protocols include: (i) hand-premixed mixtures, which was produced by shaking in a glass jar; (ii) mixtures prepared by stirring in supercritical CO_2 at 14.8 MPa and 35 C, but not subjected to REHPS; (iii) 1-pass REHPS of the hand premix; (iv) 1-pass REHPS of the stirring premix; and (v) 2-pass REHPS, where protocol iii was used as the premix. It is clear from the first row of data in Table 1 that stirring offered a small improvement in the average IOS value over hand mixing, but it improved significantly the sample-to-sample reproducibility. Figure 5 shows the superimposed elemental scans of alumina (white, or green in color online) and silica (black, or blue in color online) from typical elemental mappings obtained through EDS for the 50:50 hand-mixing, 72:28 hand-mixing, and 50:50 stirred premixed powders (protocols i, ii). White areas (green in color online) represent an abundance of alumina, whereas black areas (blue in color online) represent an abundance of silica. Figure 5a and b clearly shows the inhomogeneity on the scale of 10s of microns, whereas Fig. 5c depicts inhomogeneity only at a smaller scale. The corresponding SOS values were 15, 18, and 5 μm, respectively. This confirms that mixing was improved by stirring.

Figure 6 shows superimposed elemental scans for the 72:28 mixtures after the REHPS process. The hand-premixed 72:28 powder mixture that exited the chamber (unit 5, Fig. 1) during expansion, but did not pass through the nozzle (i.e., remained in the connecting tubing between the vessel and the nozzle), was shown

Table 1 Intensity of segregation ($\times 10^{-3}$) of various alumina–silica mixing protocols including: (i) hand-premixed mixtures, (ii) mixtures prepared by stirring, (iii) 1-pass REHPS of the hand premix, (iv) 1-pass REHPS of the stirring premix, and (v) 2-pass REHPS mixtures

Mixing condition	Pressure (MPa)	Temp (C)	1-pass REHPS			2-pass REHPS	
			50:50 Hand mixed	50:50 Stirred Mixed	72:28 Hand Mixed	50:50	72:28
Premix without REHPS	–	–	320 ± 90	160 ± 100	160 ± 80	–	–
Gas	1.72	45	13 ± 17	2.6 ± 0.1	5.5 ± 6.2	2.4 ± 0.5	2.4 ± 1.1
	2.76		12 ± 10	2.5 ± 0.5	4.5 ± 2.2	–	–
	5.51		5.4 ± 3.4	2.7 ± 0.6	8.7 ± 6.7	–	–
Supercritical	7.93		6.8 ± 6.8	1.6 ± 0.2	3.8 ± 1.5	2.3 ± 0.5	1.9 ± 1.2
	11.03		8.5 ± 4.4	4.0 ± 2.0	8.3 ± 8.1	–	–
	13.79		4.3 ± 2.5	1.9 ± 0.4	10 ± 9	3.3 ± 0.7	2.9 ± 0.4
Liquid	8.27	28	4.2 ± 2.0	3.7 ± 2.0	3.9 ± 0.7	2.1 ± 0.7	1.9 ± 0.6

The first row summarizes results obtained for mixtures that were obtained either by simple hand-mixing/shaking (0.75 g of powders in a 65-mL glass jar) or stirring (a 7.0 g of powders at 2,000 RPM with a 4–2.54-cm blade rotor in supercritical CO_2 at 14.8 MPa and 35 C in a 1.5-L stainless steel vessel), but not subjected to REHPS. Other rows report results obtained after 1-pass REHPS and 2-pass REHPS from various mixing pressure and temperatures. Gas, supercritical, and liquid in the first column refer to the state of CO_2 in the chamber upstream of the nozzle

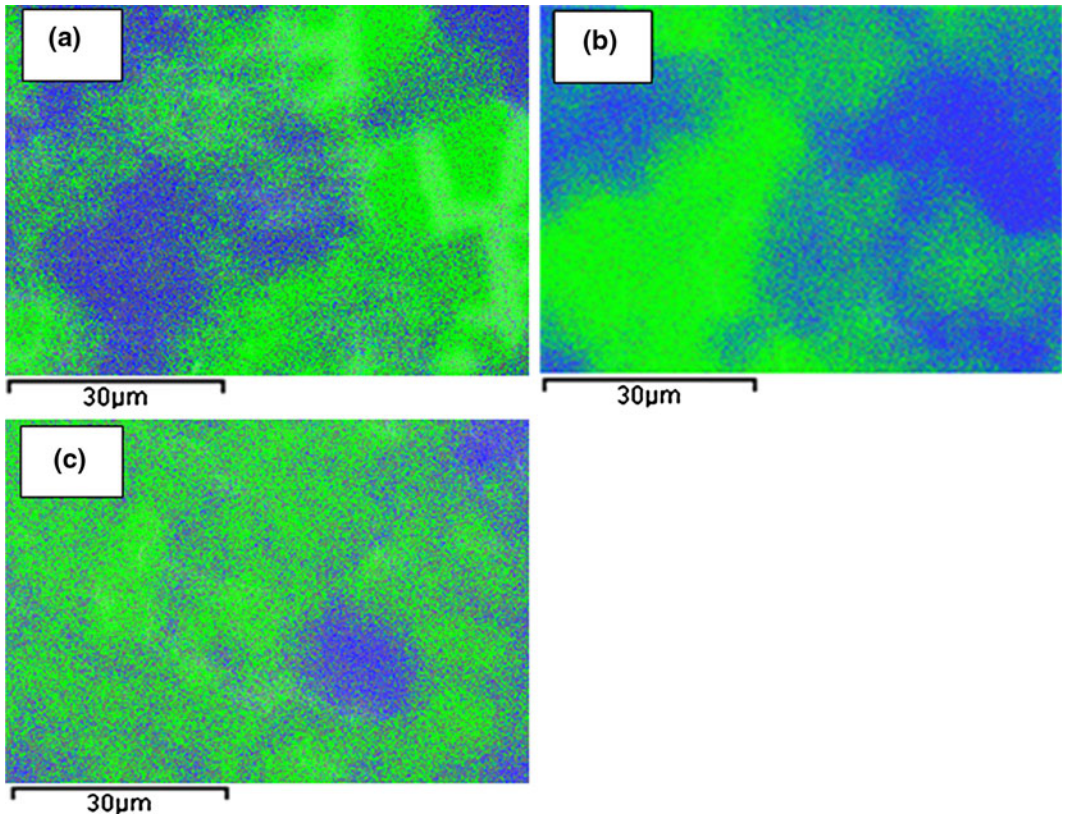

Fig. 5 Superimposed EDS scans of elemental Al (*green*) and Si (*blue*) of (a) 50:50 hand-mixed, (b) 72:28 hand-mixed, and (c) stirred premixed powders before the REHPS process. (Color Þgure online)

to produce signiÞcantly poorer-mixing quality than the REHPS process; its IOS was measured to be 0.215; the corresponding elemental mapping shown in Fig. 6a is only slightly better than that shown in Fig. 5b. This conÞrmed that the deagglomeration and subsequent mixing principally occurred in the nozzle or further downstream. The EDS scans obtained for 1-pass and 2-pass REHPS mixed powders are shown in Fig. 6b and c; it is readily apparent that they are far superior to the samples not processed through REHPS. It should be noted that the spatial variations seen in these two panels are close to or less than the resolution limit of the instrument resulting in SOS values that are not meaningful. Therefore, IOS was used to compare the REHPS mixtures. For the hand-premixed powder, 2-pass REHPS (Fig. 6c) appears to yield a slightly superior mixing than 1-pass REHPS (Fig. 6b), as already noted in Table 1.

The samples produced through REHPS did manifest appreciable variability (as evidenced by the 95% conÞdence limits shown in Table 1); nevertheless, all the samples were markedly superior to the samples that were not processed through REHPS. Some of these results are shown graphically in Fig. 7, which depicts the intensity of segregation from various mixing protocols (iii, iv, and v) and indicates that REHPS of the stirred premixed powders signiÞcantly improved the mixing quality and decreased the variability (when compared to that seen for the 1-pass hand-premixed REHPS mixture). The superior IOS obtained for the REHPS of stirred and 2-pass REHPS mixtures in comparison to the hand-premixed mixtures indicates that improved premixing signiÞcantly enhances the REHPS process. Better mixing before entering the nozzle facilitates simultaneous deagglomeration of aggregates of individual constituents during ßow through the nozzle and subsequent intimate mixing before reagglomeration occurs. Conversely, with poor premixing, simultaneous deagglomeration of aggregates of individual constituents

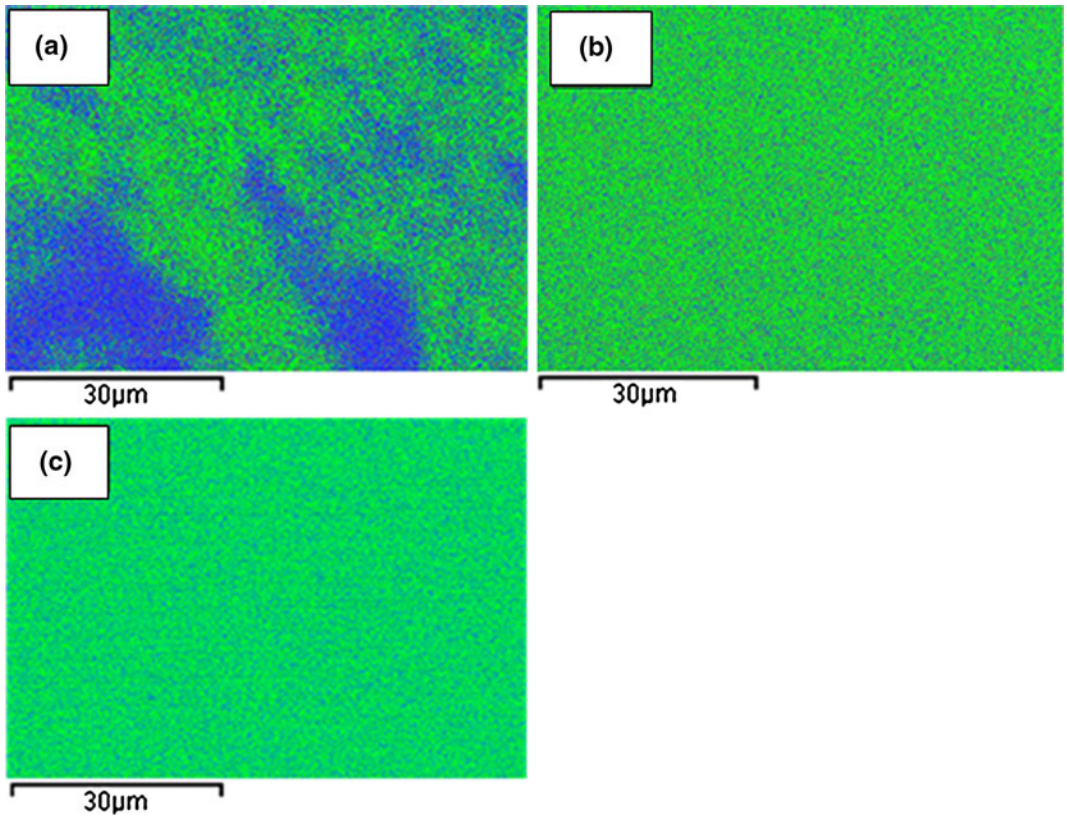

Fig. 6 Superimposed EDS scans of elemental Al (*green*) and Si (*blue*) of (a) the hand-mixed powders that remained in the connecting tubing between the high-pressure vessel and the expansion nozzle, b (1) 1-pass, and c (2) 2-pass REHPS-mixed powders. Alumina:silica weight ratio = 72:28. Sample expanded from 7.93 MPa and 45 C. (Color figure online)

occurs to a lesser extent, resulting in diminished intimate mixing. It should be noted that 1-pass stirred premixed REHPS was comparable to 2-pass hand-premixed REHPS, so stirred premixing minimizes the need for a time-intensive second pass.

It is expected that the improved deagglomeration that was shown to occur as pressure increases toward 7.93 MPa also improves mixing; however, the effect of poor axial mixing could introduce variability. This variability could minimize the expected mixing enhancement. The sample-to-sample variability was high for REHPS mixtures expanded from pressures greater than 7.93 MPa in comparison to expansion from lower pressures conditions; this is attributed to the formation of dry ice and its adverse effect on deagglomeration.

To probe the influence of nozzle diameter on the quality of mixing, experiments were also carried out using 508- and 1,524-μm diameter nozzles and 72:28 alumina–silica hand-premixed nanopowders; in all cases, the powders were expanded from 7.93 MPa and 45 C, as these conditions were found to yield (for the 254-μm diameter nozzle) both high-quality mixtures and high reproducibility. Figure 6a and b shows the EDS scans for the REHPS mixtures produced with the 508- and 1,524-μm nozzles, respectively. Comparison of these elemental maps to those produced by expansion through a 254-μm nozzle, shown in Fig. 6b, clearly indicates that increasing the nozzle diameter adversely affects the level of homogeneity. Table 2 summarizes the IOS and SOS results for expansion through the three different nozzles. Table 2 also lists the size of the most energetic eddies, which has been predicted to be dependent on the Reynolds number, Re, and the nozzle diameter (also tabulated), d_{nozzle}, according to Eq. 4 (Perry and Green 2009):

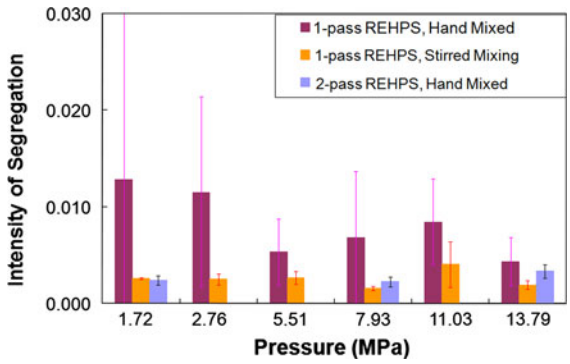

Fig. 7 IOS values for alumina–silica mixtures (50–50 wt%) expanded from different pressures through a 254-μm nozzle. The results are shown for mixtures prepared in three different ways: hand-premixed 1-pass REHPS, hand-premixed 2-pass REHPS, and stirred-premix 1-pass REHPS. See Table 1 for more details about the mixing conditions

$$L_e = 0.05 D_{\text{nozzle}} \text{Re}^{-1/8}. \quad (4)$$

These eddy length scales were calculated using the pressure and temperature predictions for choked flow conditions of a perfect gas (Shapiro 1953) and other physical data from the National Institute of Standards and Technology (Lemmon et al. 2009). The intensity of segregation increased nearly quadratically with nozzle diameter, whereas the scale of segregation varied nearly linearly with nozzle diameter. The close correspondence with the eddy length and SOS is striking; it suggests that the most energetic eddies present in the flow through the nozzle played an important role in the deagglomeration and mixing processes. This suggests that the shear-induced deagglomeration (examined by To et al. 2009) plays an important role in the deagglomeration and mixing process; however, our results differ from those of To et al in a significant way. The model presented in To et al. analyzed the role of gradients in the time-averaged velocity field, whereas our results indicate that the deagglomeration is closely tied to the most energetic eddies.

The impaction of the agglomerates with the Mach disk located downstream of the nozzle exit can also play a role in the deagglomeration and mixing processes. The results presented in Table 2 do not discount the contribution of the impact deagglomeration; as the EDS analysis is a volume-sampling method, it emphasizes the presence of large agglomerates, whose size (according to our results) appears to be closely tied to the action of the eddies. This suggestion comes at least in part from the fact that only about 50% of the agglomerates pass through the Mach disk (To et al. 2009). The remainder of the agglomerates is likely to flow around the Mach disc and pass through much weaker oblique shocks.

Mixtures at mullite stoichiometry were fired at 1,400 °C for 1 h at a heating rate of 20 °C/min. The conversion of alumina and silica to mullite was determined through quantitative XRD. It is briefly noted that hand-mixed powders reached 43.4% mullitization, whereas 2-pass REHPS mixed samples (expanded from 1.72 MPa) resulted in 82.0%

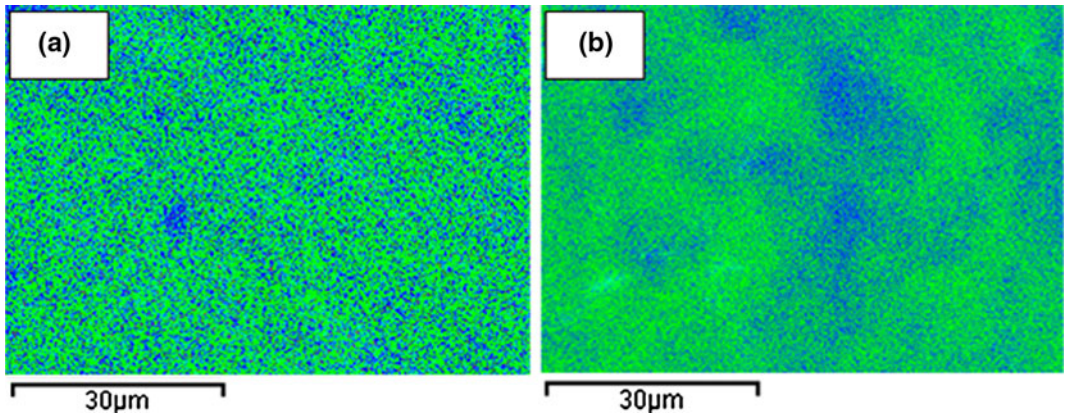

Fig. 8 Superimposed EDS scans of elemental Al (*green*) and Si (*blue*) for 1-pass REHPS through nozzles with different diameters: **a** 508 μm and **b** 1,524 μm. The EDS elemental scan for the 254-μm nozzle is shown in Fig. 6b. Alumina:silica weight ratio = 72:28. Samples expanded from 7.93 MPa and 45 °C. (Color figure online)

Table 2 Intensity of segregation (IOS), scale of segregation (SOS), carrier fluid Reynolds number, and length scale of the most energetic eddies during REHPS flow through the nozzles of different diameters. Mullite (72:28) mixtures were expanded from 7.93 MPa and 45C. This data coincide with Figs. 6b and 8a and b

Nozzle ID (μm)	IOS	Scale of segregation (μm)	Reynolds number	Max energy eddy length (μm)
254	0.0038	<2	0.99 (10^6)	2.3
508	0.0152	4.3	2.0 (10^6)	4.1
1,524	0.1405	10.9	6.0 (10^6)	10.8

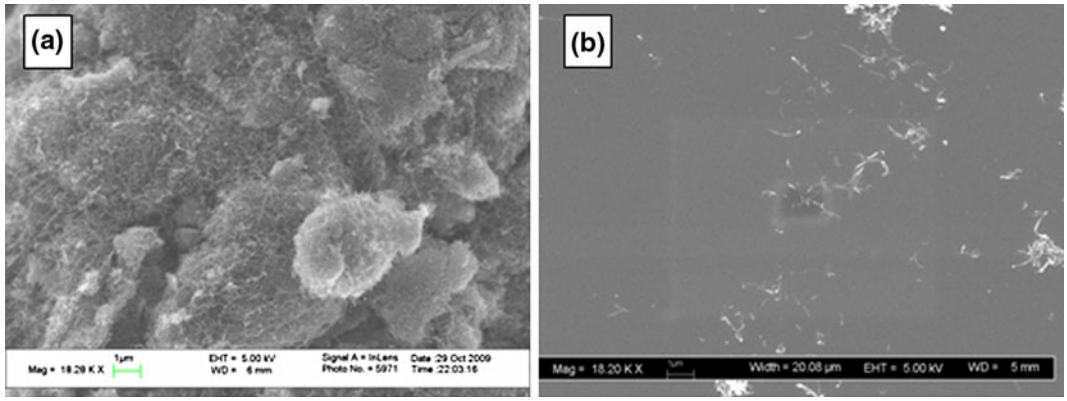

Fig. 9 SEM images of carbon nanotubes (a) before and (b) after deagglomeration through the REHPS process. The sample was expanded from 7.93 MPa and 45C

mullitization. This significant increase in the extent of mullitization further confirms a significant improvement in mixing quality (which has a direct bearing on the mullitization reaction extent readily achievable without need for extensive diffusion or viscous flow under reaction conditions) afforded by REHPS.

Deagglomeration and mixing of carbon nanotubes

Sanganwar et al. have previously shown that ultrasonic mixing in supercritical fluids, although highly capable of mixing spherical nanopowders together, was unable to loosen the tight carbon nanotube bundles (Sanganwar et al. 2008). This difficulty likely stems from the high aspect ratio and strong interactions between the nanotubes. This prompted a brief study on the quality of deagglomeration of dry CNT agglomerates afforded by REHPS. Figure 9a and b shows SEM images of CNT agglomerates before and after REHPS deagglomeration from 7.93 MPa and 45 C. It can be seen that the unprocessed CNT formed large agglomerates (generally >10 μm or larger), whereas the REHPS-deagglomerated CNT were much smaller in size. Figure 10 shows the size distribution (in terms of Feret diameter) for the REHPS-deagglomerated CNT, which are predominately in the submicron range.

We also examined the quality of mixing of CNT with alumina, silica, and titania nanopowders attainable through REHPS. The high aspect ratio of CNT makes it easier to distinguish CNT from the other constituent in the mixture and evaluate the quality of mixing simply from image analysis. Figure 11a–c presents representative images obtained in this mixing study and shows clearly that REHPS has been able to provide mixing at submicron scale. Figure 11a shows silica agglomerates (a few hundred nanometers in size) integrated into micron-sized CNT agglomerates. Figure 11b and c shows analogous results for the CNT-titania and CNT-alumina systems. Some differences seen in these three systems are likely to be related to the interaction between the constituents: CNT and silica (silane-coated) are both hydrophobic, whereas titania and alumina are both hydrophilic, which likely made CNT and silica more amenable to mixing.

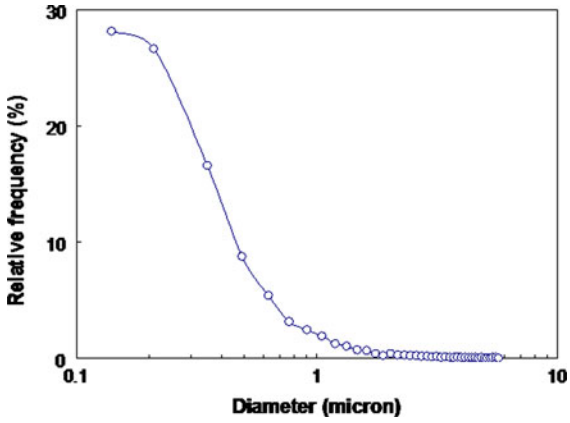

Fig. 10 Size distribution obtained through image analysis of REHPS-deagglomerated CNT

Concluding remarks

REHPS, an environmentally benign approach that produces dry powders, was studied for producing mixtures of nanopowders with a scale of segregation on the order of a few microns or smaller. In this study, two characterization methods having better resolution capabilities than those used in previous studies by Wei et al. (2002) and Yang et al. (2003) were used to analyze the mixing quality of the REHPS-processed samples. First, the constituent concentration was determined at 400 sites on the surface of pressed pellet using EDS–SEM to determine the intensity of segregation. Second, an elemental mapping of alumina was obtained through EDS–SEM analysis to determine the scale of segregation, which could be correlated to agglomerate size, thus permitting a physical interpretation of the mixing quality. Employing more rigorous mixing characterization and experimental protocols than those used in the previous studies, we examined the influence of the expansion nozzle size, quality of premixing of the constituent materials, and preexpansion pressure on deagglomeration and mixing

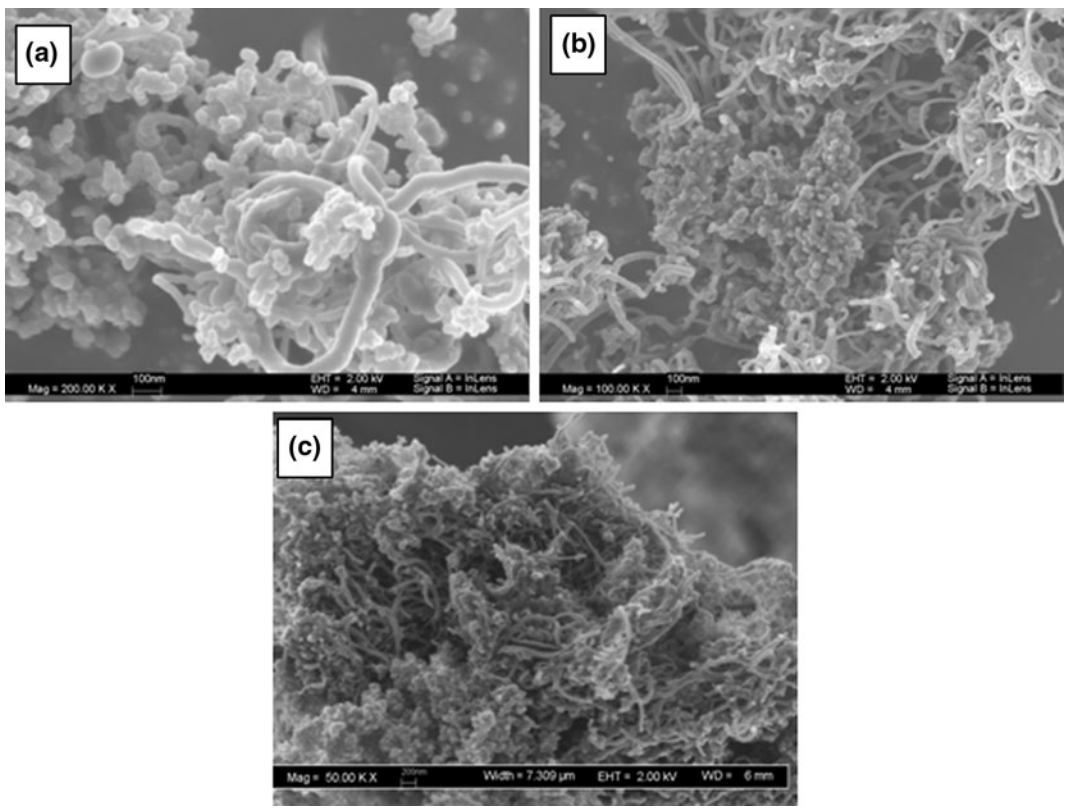

Fig. 11 Scanning electron micrographs of mixtures of carbon nanotubes and (a) silica, (b) titania, and (c) alumina nanopowders obtained through the REHPS process. Samples were expanded from 7.93 MPa and 45 °C. Mixing at submicron scale is clearly evident. Scale bars denote 100, 100, and 200 nm for images a, b, and c, respectively

attained through REHPS. The effect of premix quality was examined by using feed nanopowders that were (a) hand mixed, (b) stirred in a supercritical ßuid, or (c) previously processed through REHPS. The two principal results of this study are as follows.

First, it is demonstrated that the quality of premixing of the agglomerates of the individual constituents before transport through the nozzle had a measurable inßuence on the intensity and scale of segregation observed with REHPS-processed mixtures. Improved premixing through stirring in the supercritical chamber before expansion through nozzle was found to be very beneÞcial. Single-pass REHPS processing of stirred mixtures produced mixing quality values that were as good as the 2-pass REHPS processing of hand-mixed samples. Improved premixing also improved the reproducibility of the results.

Second, our analysis of the REHPS deagglomeration results indicates that shear associated with the energetic eddies inside the nozzle plays an important part in the deagglomeration of the nanopowders. More speciÞcally, the average size of deagglomerated fragments decreased with increasing upstream pressure, similar to those previously observed (To et al. 2009); and a decrease in nozzle diameter led to improved mixing quality as indicated by a nearly linear decrease in scale of segregation and a nearly quadratic decrease in intensity of segregation. It is also shown that the fragment sizes correlate well with the length scale of the maximum energy eddies.

Two potential applications of REHPS for creating nano-composites are also illustrated. In the Þrst example, it is shown that improved mixing of the alumina and silica nanopowders through REHPS led to improved extent of mullite formation during high-temperature reactions. In the second example, it is shown that REHPS can be used to deagglomerate the carbon nanotube bundles and mix them at submicron scale; to the best of our knowledge, this is the Þrst demonstration that REHPS can be used effectively to deagglomerate nanotube bundles and mix them with other ingredients at submicron scale.

Acknowledgments This study was supported in part by the National Science Foundation through a Nano-Interdisciplinary Research Team (NIRT) grant, DMI-0506722, and an IGERT fellowship to Daniel To through DGE-0504497. Partial support from EEC-0540855 to Rajesh Dave and Daniel To is also acknowledged.

References

Adamson TC, Nicholls JA (1959) On the structure of jets from highly underexpanded nozzles into still air. J Aerospace Sci 26:16Ð24

Ammednola P, Chirone R (2010) Aeration and mixing behaviours of nano-sized powders under sound vibration. Powder Technol 201:49Ð56

Baldyga J, Orciuch W, Makowski L, Malski-Brodzicki M, Malik K (2007) Break up of nano-particle clusters in high-shear devices. Chem Eng Process 46(9):851Ð861

Brandt O, Rajahusmi AM, Roth P (1987) First observations on break up of particle agglomerates in shock waves. Exp Fluids 5:86Ð94

Danckwerts PV (1952) The deÞnition and measurement of some characteristics of mixtures. Appl Sci Res 3:279Ð296

Duncan MA, Rouvray DH (1989) Microclusters. Sci Am 261:110Ð115

Endo Y, Hasebe S, Kousaka Y (1997) Dispersion of aggregates of the powder by acceleration in an air stream and its application to the evaluation of adhesion between particles. Powder Technol 91:25Ð30

Galinat S, Masbernat O, Guiraud C, Dalmazzone C, Noik C (2005) Drop break up in turbulent pipe ßow downstream of a restriction. Chem Eng Sci 60:6511Ð6528

Hu J, Johnston KP, Williams ROI (2004) Nano-particle engineering processes for enhancing the dissolution rates of poorly water soluble drugs. Drug Dev Ind Pharm 30(3):233Ð245

Huang C, Wang Y, Wei F (2008) Solid mixing behavior in a nano-agglomerate ßuidized bed. Powder Technol 182(3):334Ð341

Kumari L, Zhang T, Du GH, Li WZ, Wang QW, Datye A, Wu KH (2008) Thermal properties of CNT-alumina nanocomposites. Compos Sci Technol 68(9):2178Ð2183

Lemmon EW, McLinden MO, Friend DG (2009) Thermophysical properties of ßuid systems. In: Mallard WG, Linstrom PJ (eds) NIST chemistry webbook: NIST standard reference database number 69. National Institute of Standards and Technology, Gaithersburg, MD

Nakamura H, Watano S (2008) Fundamental particle ßuidization behavior and handling of nano-particles in a rotating ßuidized bed. Powder Technol 183:324Ð332

Nam CH, Pfeffer RR, Dave RN, Sundaresan S (2004) Aerated vibroßuidization of silica nano-particles. AIChE J 50:1776Ð1785

Perry RH, Green DW (eds) (2009) PerryÕs chemical engineersÕ handbook, 8th edn. McGraw-Hill, New York

Pope SB (2000) Turbulent ßows. Cambridge University Press, Cambridge, England, New York

Quevedo J, Omosebi A, Pfeffer RR (2009) Fluidization enhancement of agglomerates of metal oxide nano-powders. AIChE J 56(6):1456Ð1468

Rawle AF (2007) Micron sized nano-materials. Powder Technol 174(1Ð2):6Ð9

Sanganwar GP, Gupta RB (2008) Enhancement of shelf like and handling properties of drug nano-particles: nanoscale mixing of itraconazole with silica. Ind Eng Chem Res 47(14):4717Ð4725

Sanganwar GP, Gupta RB, Ermoline A, Scicolone JV, Dave RN (2008) Environmentally benign nanomixing by sonication in high pressure carbon dioxide. J Nanopar Res 11:405Ð419

Scicolone JV, Mujumdar A, Dave RN (2008) Mixing of nanosized particle by magnetically assisted impaction mixing in dry and ßuid suspension. In: Proceedings of AIChE 2008 Annual Meeting. Philadelphia, PA. Accessed 17 Nov 2008

Seekkuarachchi IN, Kumazawa H (2008) Aggregation and disruption mechanisms of nanoparticulate aggregates. 2. Dispersion of aggregates using a motionless mixer. Ind Eng Chem Res 47:2401Ð2413

Shapiro A (1958) The dynamics and thermodynamics of compressible ßuid ßow. Ronald Press, New York

Shieh Y-T, Liu G-L, Hwang KC, Chen C-C (2005) Crystallization, melting and morphology of PEO in PEO/MWNT-g-PMMA blends. Polymers 46:10945Ð10951

Shinohara N, Dabbs DM, Aksay IA (1986) Infrared transparent mullite through densiÞcation of monolithic gels at 1250 C. Infrared Opt Transm Mater 683:19Ð24

Sperling RA, Parak WJ (2010) Surface modiÞcation, functionalization and bioconjugation of colloidal inorganic nano-particles. Philos Trans R Soc London A 368(1915): 1333Ð1383

Strecker J, Roth P (1994) Particle breakup in shock waves studied by single particle light scattering. Part Part Syst Char 11:222Ð226

Sun J, Gao L, Jin X (2005) Reinforcement of alumina matrix with multi-walled carbon nanotubes. Ceram Int 31(6): 893Ð896

To D, Yin X, Sundaresan S, Dave RN (2009) Deagglomeration of nano-particle aggregates via rapid expansion of high-pressure suspensions. AIChE J 55(11):2756Ð3032

Valverde JM, Quintanilla MA, Catellanos A, Lepek D, Quevedo J, Dave RN, Pfeffer RR (2008) Fluidization of Þne and ultraÞne particles using nitrogen and neon as ßuidizing gases. AIChE J 54(1):86Ð103

Van der Wel PGJ (1999) Powder mixing. Powder Handl Process 11(1):83Ð86

Vankova N, Tcholakova S, Ivanov IB, Vulchev VD, Danner T (2007) EmulsiÞcation in turbulent ßow 1: mean and maximum drop diameters in inertial and viscous regimes. J Colloid Interf Sci 312(2):363Ð380

Venables HJ, Wells JI (2001) Powder mixing. Drug Dev Ind Pharm 27(7):599-612

VolÕkhin VV, Kazakova IL, Pongratz P, Halwax E (2000) Mullite formation from highly homogeneous mixtures of Al_2O_3 and SiO_2. Inorg Mater 36(4):375Ð379

Voss A, Finlay W (2002) Deagglomeration of dry powder pharmaceutical aerosols. Int J Pharm 248:39Ð50

Wei D, Dave RN, Pfeffer R (2002) Mixing and characterization of nanosized powders: an assessment of different techniques. J Nanopart Res 4:21Ð41

Weinekotter R, Gericke H (2000) Mixing of solids, particle technology series. Kluwer Academic Publishers, Dordrecht, the Netherlands

Xie L, Rielly CD, Ozcan-Taskin G (2008) Break-up of nanoparticle agglomerates by hydrodynamically limited processes. J Disper Sci Technol 29:573Ð579

Yang J, Wang Y, Dave RN, Pfeffer RR (2003) Mixing of nanoparticles by rapid expansion of high pressure suspensions. Adv Powder Technol 14:471Ð493

Zumaeta N, Cartland-Glover GM, Heffereman SP, Byrne EP, Fitzpatrick JJ (2005) Breakage model development and application with CFD for predicting breakage of whey protein precipitate particles. Chem Eng Sci 60:3443Ð3452

Zumaeta N, Byrne EP, Fitzpatrick JJ (2007) Predicting precipitate breakage during turbulent ßow through different ßow geometries. Colloid Surface A Physicochem Eng Asp 292:251Ð263